Equisetum arvense Templating of Zeolite Beta Macrostructures with Hierarchical Porosity

Valentin P. Valtchev,*,† Monique Smaihi,‡ Anne-Catherine Faust,† and Loic Vidal§

Laboratoire de Materiaux Mineraux, UMR-7016 CNRS, ENSCMu, UHA, 3 rue Alfred Werner, 68093 Mulhouse, Cedex, France, IEM, UMR-5635 CNRS-ENSCM-UM2, CNRS, 1919 route de Mende, 34293 Montpellier Cedex 5, France, and Institut de Chimie des Surfaces et Interfaces, UPR-9069 CNRS, 15, rue Jean Starcky, 68057 Mulhouse Cedex, France

Received October 31, 2003. Revised Manuscript Received January 17, 2004

Biomimetic zeolite Beta macrostructures with hierarchical porosity were prepared by using a silica-containing vegetal template (*Equisetum arvense*). Leaves and stems of *Equisetum arvense* were subjected to hydrothermal treatment with a zeolite Beta precursor solution. The zeolite readily crystallized in the vegetal tissues with the zeolite nucleation being induced by the highly reactive biomorphic silica deposited at the epidermal surface of the plant. Upon calcination the obtained zeolite/vegetal composite was transformed into a solely zeolite macrostructure that retained all morphological features of the vegetal template. The analysis of the zeolite/vegetal composite and all-zeolite replica showed that material with hierarchical porosity was obtained. The leaves and the stems of *Equisetum arvense* were transformed into micro-/mesoporous and micro-/meso-/macroporous structures, respectively. These structures were built up of zeolite nanoparticles with smaller sizes compared to the crystals from the bulk solution. Thus, the biotemplate controlled both the macromorphology and the nanolevel organization of the materials.

Introduction

Hierarchical porous structures are expected to show a better performance in areas such as heterogeneous catalysis, chromatography, and separation of biomolecules, gases, and liquids. Their presumable higher efficiency is a result of the combination of high selectivity and improved kinetics with respect to corresponding bulk materials. Various combinations of hierarchical porous structures, for example, micro-/mesoporous,[1−3] meso-/macroporous,[4−6] micro-/macroporous,[7−11] and micro-/meso-/macroporous,[12] have been synthesized by extension of the template strategy that was first employed for the synthesis of microporous zeolite-type materials.[13] Small organic molecules used in the synthesis of zeolitic materials have been substituted by surfactant micelles to synthesize organized mesoporous materials[14] and lately by arrays of uniform spheres for the preparation of macroporous solids with monomodal pore size distribution.[15,16] The utilization of templates with specific macromorphological features would allow the control of both the shape and the size of the solid. Although some morphological constructions with hierarchical porosity, for example, beads,[2] have been obtained with synthetic templates, the morphological features of these materials are far from being controlled. Therefore, templates that could provide a specific macromorphology with hierarchical organization at the nanolevel scale are highly desirable. The ability to combine complex morphology with hierarchical architecture is typical of biological specimens. Examples of the transformation of such specimens into inorganic structures are also provided by nature, for example, the process of petrification in which a supersaturated mineral containing solution precipitates within the interstices of the plant filling them with the mineral.[17] After the decay of the organic tissue a negative replica

* Corresponding author. E-mail: V.Valtchev@uha.fr.
† UMR-7016 CNRS, ENSCMu, UHA.
‡ UMR-5635 CNRS-ENSCM-UM2.
§ UPR-9069 CNRS.

(1) Wang, H.; Wang, Z.; Huang, L.; Mitra, A.; Holmberg, B.; Yan, Y. *J. Mater. Chem.* **2001**, *11*, 2307.
(2) Tosheva, L.; Valtchev, V.; Sterte, J. *Microporous Mesoporous Mater.* **2000**, *35−36*, 621.
(3) Liu, Y.; Pinnavaia T. J. *Chem. Mater.* **2002**, *14*, 3.
(4) Velev, O. D.; Tessier, P. M.; Lenhoff, A. M.; Kaler, E. W. *Nature* **1999**, *401*, 548.
(5) Lebeau, B.; Fowler, C. E.; Mann, S.; Farcet, C.; Charleux, B.; Sanchez, C. *J. Mater. Chem.* **2000**, *10*, 2105.
(6) Yu, C.; Tian, B.; Fan, J.; Stucky, G. D.; Zhao, D. *Chem. Lett.* **2002**, 62.
(7) Lee, Y.-J.; Lee, J. S.; Park, Y. S.; Yoon, K. B. *Adv. Mater.* **2001**, *13*, 1259.
(8) Holland, B. T.; Abrams, L.; Stein, A. *J. Am. Chem. Soc.* **1999**, *121*, 4308.
(9) Valtchev, V. *J. Mater. Chem.* **2002**, *12*, 1914.
(10) Wang, Y. J.; Tang, Y.; Ni, Z.; Hua, W. M.; Yang, W. L.; Wang, X. D.; Tao, W. C.; Gao, Z. *Chem. Lett.* **2000**, 510.
(11) Zhu, G.; Qin, S.; Gao, F.; Li, D.; Li, Y.; Wang, R.; Gao, B.; Li, B.; Guo, Y.; Xu, R.; Liu, Z.; Terasaki, O. *J. Mater. Chem.* **2001**, *11*, 1687.
(12) Rhodes, K. H.; Davis, S. A.; Caruso, F.; Zhang, B.; Mann, S. *Chem. Mater.* **2000**, *12*, 2832.
(13) Szostak, R. *Molecular Sieves*, 2nd ed.; Blackie Academic & Professional: London, 1998; p 359.
(14) Vartuli, J. C.; Roth, W. J.; Beck, J. S.; McCullen, S. B.; Kresge, C. T. In *Molecular Sieves: Science and Technology, Vol. I*; Karge, H. G., Weitcamp, J., Eds.; Springer: Berlin, 1998; p 97.
(15) Velev, O. D.; Keler, E. W. *Adv. Mater.* **2000**, *12*, 531.
(16) Stein, A. *Microporous Mesoporous Mater.* **2001**, *44−45*, 227.
(17) Iler, R. K. In *The Chemistry of Silica*; John Wiley & Sons: New York, 1979; p 88.

10.1021/cm035100t CCC: $27.50 © 2004 American Chemical Society
Published on Web 03/09/2004

of the biological structure is obtained. This process, however, is long and difficult to completely reproduce under laboratory conditions. Nevertheless, biological structures, namely plants, have been successfully used as templates for the preparation of biomorphic ceramics.[18,19] These preparations include deposition of an amorphous precursor on the surface of the plant followed by a high-temperature treatment, which results in the formation of a ceramic structure and volatizes the biotemplate.

Microporous zeolite-type crystalline solids are generally synthesized under mild hydrothermal conditions. Under such conditions, to the best of our knowledge, direct laboratory zeolitization of biological templates has not been reported. Obviously, a serious obstacle for the in situ zeolitization of biological specimens is the incompatibility between the organic substrate and the inorganic zeolite precursors. Two approaches have been developed to overcome the incompatibility between the organic support and the inorganic precursors yielding porous solids: (i) presynthesized microporous nanoparticles have been assembled on the biological supports and (ii) the crystallization on the biotemplate has been induced by zeolite seeds initially adsorbed on the support, which upon hydrothermal treatment with a fresh synthesis solution grow into a dense zeolite layer. The first approach has been employed for the preparation of micro-/macroporous zeolite fibers, produced by infiltration of zeolite nanocrystals into the ordered void spaces of bacterial treads,[20] and spongelike monoliths produced by starch gel templating.[21] Seeding of the support prior to hydrothermal treatment has been applied to crystallize zeolite layers on wood templates.[22] Seeds have also been used to induce zeolite formation on fossilized silica shells of single-cell algae (diatoms).[23,24] These approaches ensure replication of large surfaces accessible to zeolite seeds, that is, the macromorphological features of the biotemplate. However, a faithful zeolitization of the microarchitecture of the plant structure would not be achieved if the zeolite crystallization process did not take place within the plant tissue, thus resembling the petrification of biological cells in nature.[17] Such an opportunity is offered by some plants, for example, the ones from the *Equisetaceae* family, whose members are rich in amorphous silica[25] where deposition occurs at discrete knobs and rosettes at the epidermal surface.[26] Very recently, it was found that biogenic silica deposited in the epidermal surface of *Equisetum arvense* promotes zeolite crystallization.[27] This opened up routes for faithful laboratory zeolitization of silica-containing fresh plants yielding advanced porous materials.

The objective of the present study was to demonstrate that the different parts of the silica-containing plant *Equisetum arvense* can play a dual role; that is, the plant can control both the organization of the inorganic material on a nanolevel scale and its macromorphological features. The feasibility of this approach was exemplified by the syntheses of zeolite Beta macrostructures using stems and leaves of *Equisetum arvense*.

Experimental Section

Equisetum arvense was collected from the campus of the University of Haute Alsace (Mulhouse, France). Prior to hydrothermal treatment, the plant was dried at least for several weeks under ambient conditions.

The syntheses of zeolite Beta on *Equisetum arvense* were performed from a clear solution prepared by dissolution of aluminum isopropoxide (Fluka) in tetraethylammonium (TEA) hydroxide (20 wt % in water, Merck). The obtained clear solution was mixed with colloidal silica sol (30 wt % in water, Merck). The resulting mixture had the following molar composition: 0.3:4.5:0.5:25:430 Na_2O:$(TEA)_2O$:Al_2O_3:SiO_2:H_2O. The presence of Na_2O in this composition is a consequence of the use of silica sol as a silica source. The syntheses were performed at 100 and 150 °C for periods of time between 1 and 20 days. After the synthesis, the zeolite/vegetal composite was separated from the zeolite crystallized in the bulk solution, treated in distilled water under ultrasonic radiation for 10 min to separate loosely attached crystals, and dried at 60 °C overnight. A part of the product was calcined at 600 °C for 5 h.

The procedure described in ref 28 was adapted for the purpose of the present study to extract the TEA template from the zeolite Beta crystallized in the plant tissues. The as-synthesized composite (0.2 g) was treated under reflux with 0.1 M acetic acid (150 mL) at 80 °C for 12 h. After the treatment, the zeolite/fiber composite was washed with distilled water and dried at room temperature.

The particle size analysis of the zeolite nanocrystals crystallized in the bulk solution was performed with a HPPS ET (Malvern) particle analyzer. Zeolite/vegetal composite and calcined materials were characterized by powder X-ray diffraction (XRD) with a STOE STADI-P diffractometer in Debye−Scherrer geometry equipped with a linear position-sensitive detector (6° in 2θ) and employment of Ge monochromated Cu $K\alpha_1$ radiation. Micrographs of the samples were taken on a Philips XL 30 LaB_6 scanning electron microscope (SEM). The zeolite particles crystallized in the tissues of the vegetal template were studied by transmission electron microscopy (TEM, Philips CM200) operating at 200 kV and using a LaB_6 crystal as an electron source. The combined TG/DTA analysis of the samples was performed with a Setaram TG-ATD *LABSYS* thermal analyzer at a heating rate of 5 °C min^{-1} in an atmosphere containing 80% N_2 and 20% O_2. Small-angle X-ray scattering (SAXS) experiments were made with an instrument having an incident wavelength equal to 0.154 nm (Cu $K\alpha_1$ radiation) using a high-resolution Bonse-Hart camera. The monochromator was a three-reflection channel-cut scattered beam. These experimental parameters allowed studies in a range of wave vectors Q from 0.02 to 1 nm^{-1}.

Nitrogen adsorption measurements were carried out with a Micromeritics ASAP 2010 surface area analyzer. The as-synthesized and calcined samples were analyzed after outgassing at 130 and 350 °C, respectively. The macropore volume was studied with a mercury Porosimeter 2000 (Carlo Erba) working in the pressure range 0.1−1000 MPa.

Results and Discussion

The inconspicuous, scalelike, whorled 30−60-mm long dried leaves were cut into pieces of 10−20 mm and

(18) Sieber, H.; Hoffmann, C.; Kaindl, A.; Greil, P. *Adv. Eng. Mater.* **2000**, *2*, 105.
(19) Shin, Y.; Liu, J.;. Chang, J. H.; Nie, Z.; Exarhos, G. J. *Adv. Mater.* **2001**, *13*, 728.
(20) Zhang, B.; Davis, S. A.; Mendelson, N. H.; Mann, S. *Chem. Commun.* **2000**, 781.
(21) Zhang, B.; Davis, S. A.; Mann, S. *Chem. Mater.* **2002**, *14*, 1369.
(22) Dong, A.; Wang, Y.; Tang, Y.; Ren, N.; Zhang, Y.; Yue, Y.; Gao, Z. *Adv. Mater.* **2002**, *14*, 926.
(23) Anderson, M. W.; Holms, S. M.; Hanif, N.; Cundy, C. S. *Angew. Chem., Int. Ed.* **2000**, *39*, 2707.
(24) Wang, Y.; Tang, Y.; Dong, A.; Wang, X.; Ren, N.; Gao, Z. *J. Mater. Chem.* **2002**, *12*, 1812.
(25) Berterma, R.; Tacke, R. Z. *Naturforsch., B: Chem. Sci.* **2000**, *55*, 459.
(26) Kaufman, P. B.; Wilber, W. C.; Schmid, R.; Najati, N. S. *Am. J. Bot.* **1971**, *58*, 309.
(27) Valtchev, V.; Smaihi, M.; Faust, A.-C.; Vidal, L. *Angew. Chem., Int. Ed.* **2003**, *42*, 2783.
(28) Jones, C. W.; Tsuji, K.; Takewaki, T.; Beck, L. W.; Davis, M. E. *Microporous Mesoporous Mater.* **2001**, *48*, 57.

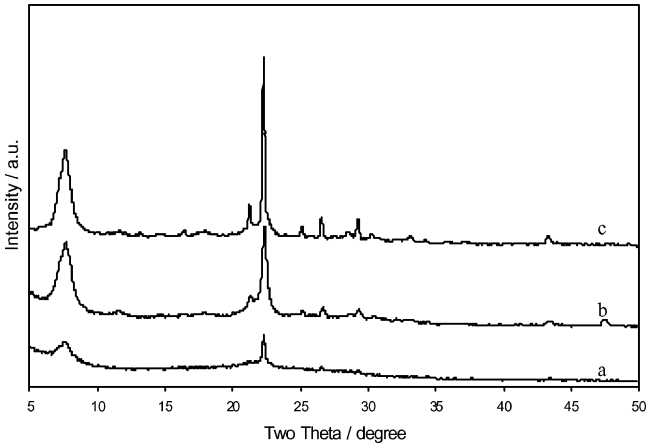

Figure 1. X-ray diffraction patterns of zeolite Beta/*Equisetum arvense* composites synthesized at 100 °C (a) and 150 °C (b) and pure zeolite Beta (c) synthesized from the same synthesis mixture at 150 °C.

subjected to hydrothermal treatment in the zeolite precursor system. Neither seed adsorption nor any chemical treatment was performed on the biotemplates prior to hydrothermal synthesis. Nevertheless, the plant structure was successfully zeolitized as shown by the XRD patterns of the zeolite/plant composite. The diffractograms of zeolite Beta/*Equisetum arvense* leaves synthesized at different temperatures were similar, containing the peaks typical of the BEA-type topology and a halo emanating from the organic part of the composite (Figure 1). The halo was more pronounced in the sample synthesized at 100 °C (Figure 1a). The XRD patters of calcined *Equisetum arvense* replicas synthesized at 100 and 150 °C were similar. It is worth mentioning that the crystallization of the zeolite within the biotemplate overtook that observed in bulk solution. For example, at 100 °C the mother liquor yielded zeolite Beta after 10 days, while the crystallization on the template was accomplished within 7 days. The size of the crystals formed in the bulk solution was larger than that grown within the biotemplate, which is additional proof that the biomorphous silica promotes zeolite nucleation in the tissues of *Equisetum arvense*. Although the effect of the biotemplate on the zeolite crystallization is very pronounced, the size of the particles is also influenced by the synthesis temperature. As can be seen in Figure 2 zeolite Beta crystallites formed at different temperatures in the biotemplate differ substantially in size.

Because of the abundant nucleation, very high zeolite loading per unit mass of the material was achieved. According to the TG analysis, the zeolite content in the composite was in the range 40−60 wt % depending on the synthesis conditions. This was almost an order of magnitude higher than that achieved on wood templates by preliminary seeding of the support (6−10 wt %).[12]

The calcination of the samples transformed the composite into an all-zeolite fiberlike material. The SEM inspection of the sample showed that the zeolite replica retains the macromorphological features and details observed in the original plant (Figure 3a−d). The extremely small zeolite Beta crystallites crystallized in the plant tissues are at the resolution limit of the SEM instrument (Figure 3e,f)). These crystals are embedded in the tissue of the template, in contrast to the films grown on supports by seeding where a homogeneous layer covers the surface of the support.

The variation of the crystallization conditions produced materials with specific properties. The results of N_2 adsorption measurements on the as-synthesized and calcined zeolite replicas of *Equisetum arvense* leaves are summarized in Table 1. The hydrothermal treatment led to a substantial increase of the total Brunnauer−Emmet−Teller (BET) surface area of the samples with respect to the initial leaves (3.9 $m^2\ g^{-1}$). The 100 °C as-synthesized sample showed a very high surface area (177 $m^2\ g^{-1}$) that suggests deposition of extremely small particles in the *Equisetum arvense* tissue. The material synthesized at 150 °C possessed a much lower specific surface area, probably related to the packing of the crystals achieved at the higher temperature (Table 1). However, upon calcination it possessed higher S_{BET} and micropore area than the 100 °C sample (Table 1).

The lower micropore area of the calcined sample synthesized at 100 °C is most probably due to an uncompleted conversion into zeolite of the aluminosilicate species deposited in the biotemplate. The analysis of micropore volumes of the calcined materials obtained at 100 and 150 °C compared with the micropore volume of reference zeolite Beta sample synthesized at 150 °C from the composition used for the zeolitization of *Equisetum arvense* confirmed this conclusion. The materials synthesized at 150 and 100 °C showed 0.23 and 0.17 $cm^3\ g^{-1}$, respectively, which is lower than that of a highly crystalline BEA-type material (about 0.28 $cm^3\ g^{-1}$).[29] These values clearly indicate the presence of dense materials with low micropore volume in the replicas of *Equisetum arvense*. The adsorption/desorption isotherms of the samples of the leaf replicas synthesized at the two different temperatures are shown in Figure 4. The sample synthesized at 150 °C showed a type I isotherm characteristic of microporous zeolite-type materials (Figure 4a). In contrast to the material synthesized at 150 °C, which contained mainly micropores (Figure 4a, inset), two types of pores were detected in the sample synthesized at 100 °C. After a steep rise in the gas uptake at low relative pressures that corresponds to the filling of the micropores, an inclination of the curve with e increase in the relative pressure can be observed (Figure 2b). At high relative pressure the upward turn with a hysteresis loop is indicative of the generation of intercrystalline mesoporosity. According to the BJH pore size distribution, the major part of these textural mesopores are in the range 50−150 Å with a sharp maximum at about 80 Å (Figure 2b, inset). As mentioned above, the material synthesized at 150 °C does not contain distinctive mesopores. Indeed, the TEM investigation showed that at higher temperature densely packed larger zeolite particles were formed (Figure 2b). The mesopore volumes, 0.68 and 0.06 $cm^3\ g^{-1}$, of the materials synthesized at 100 and 150 °C, respectively, are in good agreement with the TEM investigation. Thus, the synthesis conditions can be employed to control the secondary porosity of the material.

The leaf replicas obtained upon calcination were fragile and showed a tendency to disintegrate into small

(29) Jones, C. W.; Hwang, S.-J.; Okubo, T.; Davis, M. *Chem. Mater.* **2001**, *13*, 1041.

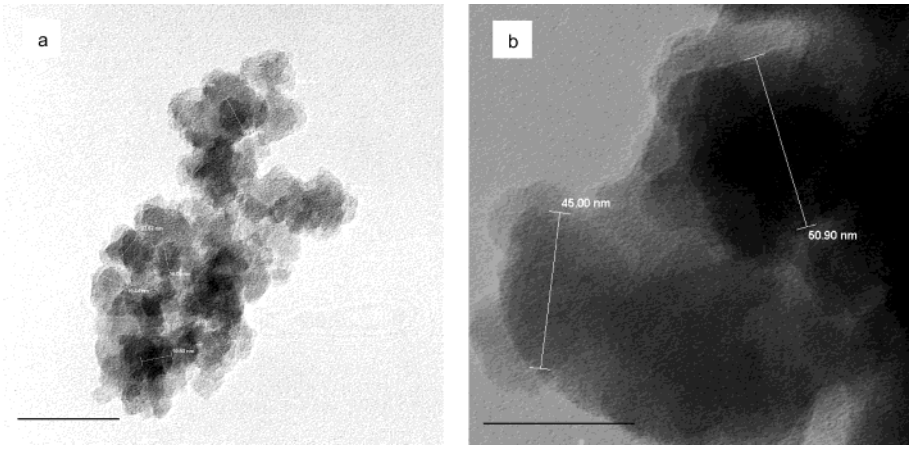

Figure 2. TEM images of zeeolite Beta particles synthesized at the *Equisetum arvense* at 100 °C (a) and 150 °C (b) (scale bar = 50 nm).

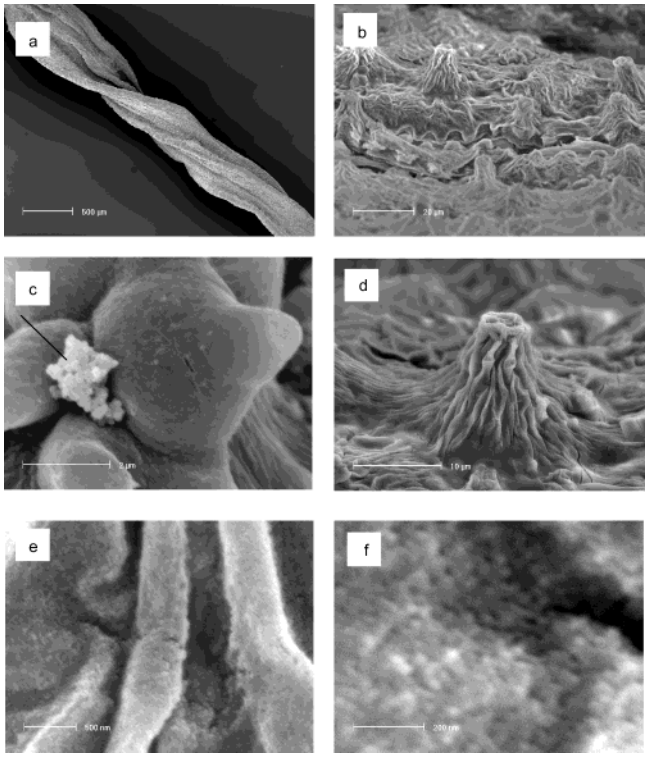

Figure 3. Low (a) and higher (b) magnification SEM views of the zeolite Beta replica of a leaf of *Equisetum arvense*. Details of the replica where the difference in the size of zeolite Beta crystallized in the synthesis solution (arrow) and at the plant tissue can be seen (c). A close view of a conic plant structure replicated by zeolite Beta (d) and the zeolite Beta replica at higher magnifications (e, f).

Table 1. Specific Surface Areas (S_{BET}) and Micropore Areas of As-Synthesized and Calcined Materials Templated by Leaves of *Equisetum arvense*

	100 °C		150 °C	
sample	as-synth.	calcined	as-synth.	calcined
S_{BET} ($m^2\ g^{-1}$)	177	465	23	527
micropore area ($m^2\ g^{-1}$)	1.3	323	0.0	466

pieces. Their mechanical properties, however, could be significantly improved by a secondary growth in a zeolite Beta precursor mixture. Alternatively, zeolite/plant composites that do not require high-temperature calcination to open the zeolite pores could be crystallized in the absence of zeolite structure-directing agents. Another feasible method that avoids high-temperature calcination is the chemical extraction of the organic structure-directing agents (SDA).[17] Zeolite Beta/*Equisetum arvense* composite synthesized at 100 °C was subjected to acetic acid treatment according to the procedure described in ref 17. After the treatment, the composite showed a substantial increase of the micropore area (167 $m^2\ g^{-1}$) with respect to the as-synthesized material (1.3 $m^2\ g^{-1}$) and retained morphological features and high flexibility of the leaves. The latter is an important characteristic of the zeolite/*Equisetum arvense* leaf composite that can be further used to tailor them into complex shapes or convert them into three-dimensional bodies by press moulding.

Further, the zeolite Beta/*Equisetum arvense* composite subjected to acid treatment was studied by SAXS and the result was compared to results for initial leaves and the as-synthesized sample (Figure 5). Dried initial leaves did not exhibit fractal behavior nor microporosity features (Figure 5a). SAXS profiles obtained for zeolitized *Equisetum arvensis* leaves (Figure 5b) contain the characteristic features of multimodal porous materials. Three Q vector domains in the ranges $Q < 5 \times 10^{-3}$ Å^{-1}, 5×10^{-3} Å$^{-1} < Q < 2 \times 10^{-2}$ Å^{-1}, and 2×10^{-2} Å$^{-1} < Q$ (Figure 5b) were observed. These Q vector domains correspond to scattering from mesopores (or small macropores), micropores, and crystallite surfaces, respectively. The slope deviation observed in the SAXS curves at 5×10^{-3} Å^{-1} in the log−log plot indicates a mean nanocrystallite size in the range 20−30 nm. Moreover, the power law behavior of the scattering intensities (i.e., a linear increase with decreasing Q with a slope equal to −4) for 2×10^{-2} Å$^{-1} < Q$ suggests that these particles have a smooth surface. These characteristic features are more pronounced after acetic acid template extraction (Figure 5c), indicating an increase of the micropore volume after the extraction procedure while the mean size of the zeolite aggregates remains constant. These results are in good agreement with the TEM observations and the N_2 adsorption measurements; that is, uniform nanoparticles and a secondary porosity were detected.

The stems of *Equisetum arvense* are hollow with walls containing smaller channels (Figure 6a), jointed with very distinct nodes. Depending on the desired size, the stems were cut into pieces and subjected to hydrother-

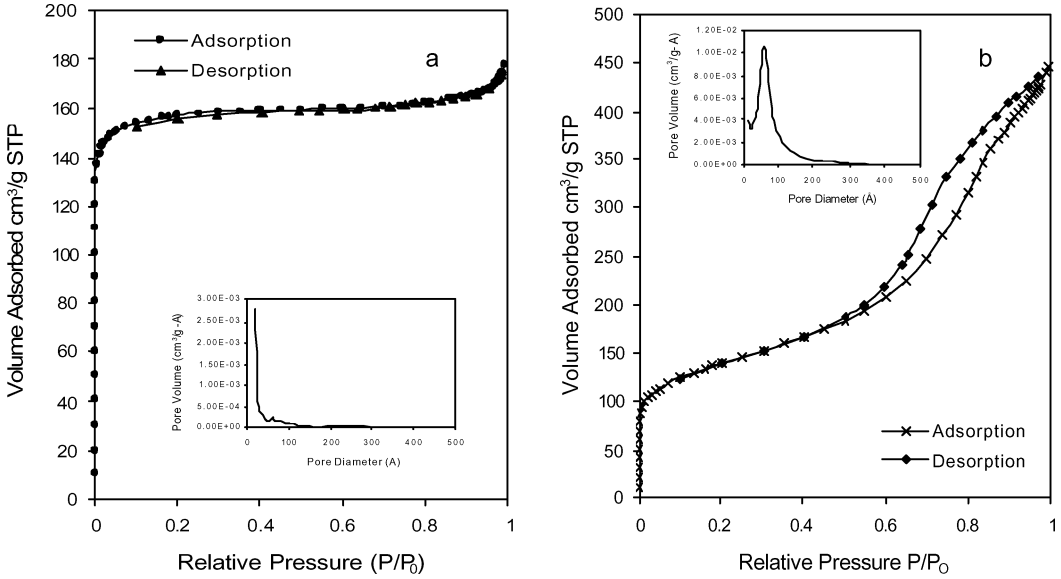

Figure 4. Adsorption/desorption isotherms for the replicas of *Equisetum arvense* leaves synthesized at 150 °C (a) and 100 °C (b). The insets represent the corresponding BJH desorption d*V*/d*D* plots.

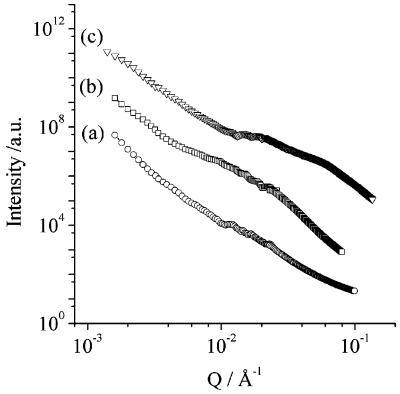

Figure 5. SAXS profiles of *Equisetum Arvense* leaves before (a) and after (b) hydrothermal treatment and after the acid extraction of the organic template (c).

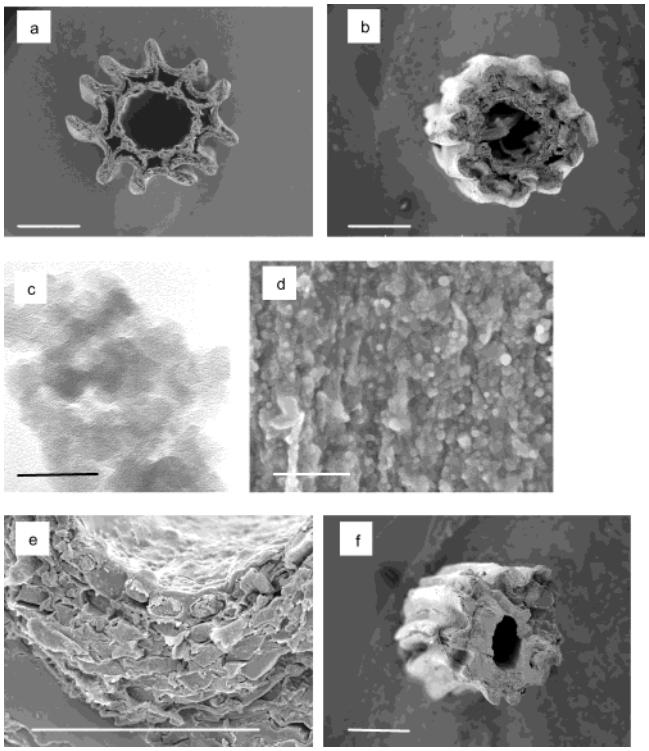

Figure 6. Cross section of a stem of *Equisetum arvense* (a) and of a stem replica with a low level of zeolite Beta loading (b) (scale bar = 1 mm). TEM image of zeolite Beta particles with lattice fringes crystallized within the plant tissue (c) (scale bar 50 nm) and a detail of the surface of tracheidal cell where larger (100−200 nm) crystals can be seen (d) (scale bar = 1 μm). Higher (e) and low (f) magnification views of zeolite Beta replica of high zeolite-loaded stem (scale bar = 1 mm).

mal treatment. It was found that the synthesis time determined the amount of zeolite crystallized within the template (Figure 6b,e). Zeolite crystallization within the tissue (20−40 nm crystals) of the biotemplate (Figure 6c) was followed by the formation of larger zeolite particles on the epidermal surface (Figure 6d) and filling with crystalline material of the small and larger canals surrounding the central hole (Figure 6e). This consecutive filling of the stem channels with zeolite may be used to control the level of zeolite loading and the meso-/macroporosity of the ultimate replica. Figure 6f represents a high zeolite-loaded stem replica where all channels except the central hole are filled. On the other hand, the mercury porosimetry showed total cumulative volumes of 962 and 462 $mm^3\ g^{-1}$ for low and high zeolite-loaded samples, respectively. These data include mainly the large mesopores and small macropores since the instrument operates at pressures over 0.1 MPa, which does not allow study of large macropores. Highly zeolite-loaded stems contained 74 wt % solid according to the TG measurements. The combined XRD/TEM/N_2 adsorption analyses showed that the deposited material was zeolite Beta with $S_{BET} = 540\ m^2\ g^{-1}$ and a micropore area of 463 $m^2\ g^{-1}$. The mechanical properties of the calcined tubular pieces were found satisfactory. The stem replicas did not show any tendency to disintegrate into smaller pieces. A certain pressure is necessary to damage the material; thus, different laboratory operations can be performed without risk of breaking the particles. The collected data showed that, after combustion of the organic tissue, the cellular structure of the stems was maintained, yielding a material with macroporous channels that can ensure high flow rate. Thus, the *Equisetum arvense* stem zeolitization resulted in a

micro-/meso-/macroporous material that retained all morphological characteristics of the plant.

Conclusions

The present study showed that fresh silica-containing plants can be transformed into materials with hierarchical porosity that retain the morphological features of the biotemplate. The various possibilities offered by the biotemplates were demonstrated by the synthesis of micro-/mesoporous and micro-/meso-/macroporous zeolite macrostructures by using leaves and stems of *Equisetum arvense* as templates, respectively. Uniform abundant nucleation of zeolite in the volume of the plant tissues induced by the biomorphic silica provided faithful replication of the plant structure and very high concentration of zeolite per unit mass of the material. The application of silica-rich biological templates may result in a large variety of morphological constructions built up of various types of zeolites and other crystalline silica-containing solids that crystallize under mild hydrothermal conditions.

The possibilities of building biomorphic materials based on biological templates are tremendous, for example, only the *Equisetaceae* family comprises about 15 members, each of them with specific morphological features and sizes varying between several centimeters and 2 m. Besides the complex morphology and multilevel organization, which at present cannot be reproduced by synthetic templates, the natural templates are environmentally benign, inexpensive, and renewable.

Although the laboratory transformation of a biological structure into mineral resembles the natural petrification, there is a substantial difference between these two processes. The laboratory zeolitization of silica-containing plants is a process providing a positive replica of the biological template due to the crystallization of the zeolite in the organic tissue. In contrast, the petrification in nature is a process where after the decomposition of the organic tissue a negative replica of the biological specimen is left behind.

Acknowledgment. V. V. is grateful to the CNRS/DFG bilateral program for financial support and Dr. L Tosheva for helpful discussion.

Supporting Information Available: Mercury porosimetry curves of high (a) and low (b) zeolite Beta-loaded *Equisetum arvense* replicas (PDF). This material is available free of charge via the Internet at http://pubs.acs.org.

CM035100T